2nd IFAC Workshop on Research, Education and Development of
Unmanned Aerial Systems
November 20-22, 2013. Compiegne, France

Inverse simulation of unconventional maneuvers for a quadcopter with tilting rotors

Irene A. Piacenza * **Fabrizio Giulietti** ** **Giulio Avanzini** ***

* *Politecnico di Torino, Department of Mechanical and Aerospace Engineering, C.so Duca degli Abruzzi 24, Turin, 10124, Italy (e-mail: irene.piacenza@polito.it)*
** *University of Bologna, Department of Mechanical and Aerospace Engineering, Via Fontanelle 40, Forlí, 47100, Italy (e-mail: fabrizio.giulietti@unibo.it)*
*** *Università del Salento, Department of Engineering, Strada per Monteroni, Lecce, 73100, Italy (e-mail: giulio.avanzini@unisalento.it)*

Abstract: An inverse simulation algorithm is applied to the determination of the control laws for tracking desired maneuvers by means of an unconventional quad-rotor configuration. This novel configuration features four rotors that are allowed to tilt around the axis of the support, thus changing the thrust vector direction in order to achieve unprecedented maneuvering capabilities. The novel configuration is compared with a conventional quad-rotor, where control moments are generated by variations of rotor rotation rates. A 90 deg roll maneuver in forward flight is also presented, to highlight the increased maneuvering capabilities of the new configuration.

Keywords: Inverse simulation, Multi-rotor, Quadrotor, Tilt-Rotor, Autonomous flight.

1. INTRODUCTION

In the last few years the study of Unmanned Vertical Take Off and Landing Vehicles (VTOL UAVs) has gained much interest. In this framework, quad-rotors and other multi-rotor configurations achieved an increasing popularity, because of their relatively simple and cheap construction and the overall low-cost involved in operating this class of platforms in various mission scenarios.

As an example, the Stanford Testbed of Autonomous Rotorcraft for Multi-Agent Control (STARMAC) quad-rotor helicopter is one of the many platforms analyzed in the literature, Hoffmann (2011). Control of the vehicle is realized for a standard configuration, where load-factor is controlled by total thrust, and lateral and longitudinal accelerations are controlled through pitch and roll angles of the aircraft. The main goal of the control is to minimize the effects of disturbances. This is demonstrated for a rather complex simulation model, where blade flapping and total thrust variation in translational flight are considered.

The work by Stingu and Lewis, where the design and manufacturing of a quad-rotor is presented, provides a simpler 6 DoF simulation model for quad-rotors, Stingu (2009). The main issue of this paper is to obtain a simple control system that successfully stabilizes a custom-built quad-rotor platform in hover, in order to have a user-friendly semi-autonomous machine.

Most of the quad-rotors found in literature are very small, with an overall mass of less than 3 kg. One of the most notable exceptions is represent by the X-4 Flyer, Pounds (2010). Also in this case the model used for simulations and the control design are both quite standard, and a PID controller is designed to stabilize the dominant decoupled pitch and roll modes.

More recent research are focused on the development of a self-stabilizing and self-navigating quad-rotor. The problem of navigation and autonomous flight for this class of vehicles, as well other VTOL UAVs, are well discussed in Kendoul (2012) and Michael (2012).

Control of a conventional quad-rotor is based on the variation of thrust developed by the four rotors, which is achieved by variations of rotor rotation rates. In hover all rotors provide equal thrust, such that the total equals vehicle weight. Two rotors turn in one direction and two in the opposite one, so that the overall yaw aerodynamic moment is cancelled (Fig. 1.a). Yawing control moments are obtained by unbalancing these aerodynamic moments by accelerating the rotors spinning in one direction and slowing down the other two. Pitch and roll moments are obtained by unbalancing the thrust of forward and rear or lateral rotors, respectively, for a conventional cruciform configuration. A variation of the rotation rate of all the rotors allows for vertical acceleration and maneuvers at a load factor greater than one.

The possibility of tilting the rotors as depicted in Fig. 1.b allows for a significantly greater flexibility in obtaining control moments. With 4 more control variables, the system becomes redundant, and it is possible to control

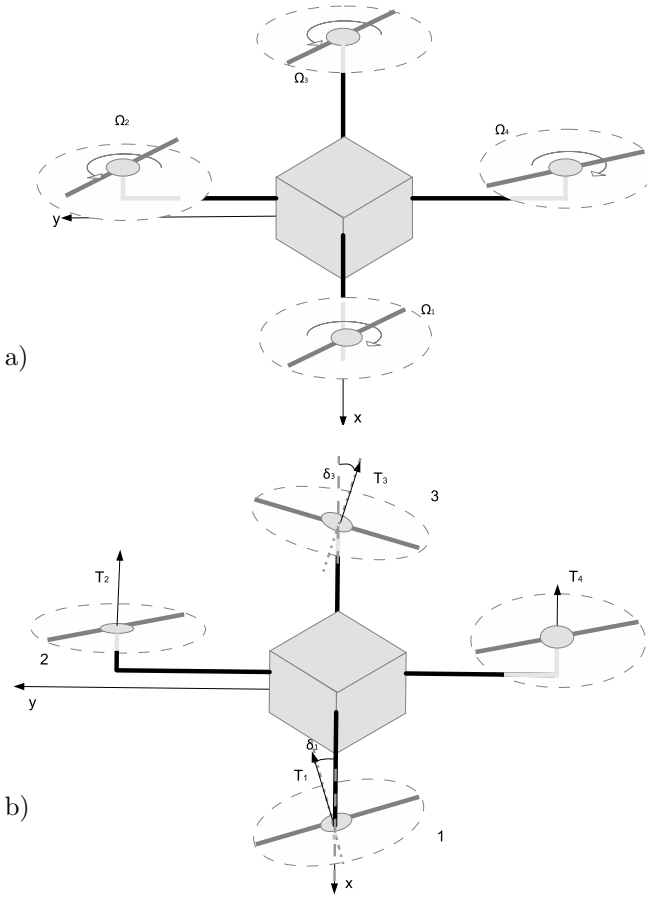

Fig. 1. Quad-rotor configurations: a) conventional; b) with tilting rotors.

flight condition simply unachievable for a conventional quad-rotor configuration with fixed propellers. A patent request has been issued for the configuration discussed in this paper, Avanzini & Giulietti (2012). As an example, it is possible to accelerate and fly in forward flight without the need for pitching the vehicle down.

A simplified model of the quad-rotor vehicle with tilting rotors is derived in the next section, which is suitable for the application of an inverse simulation technique, with the objective of proving the viability of the concept and its unprecedented maneuvering capabilities.

Inverse simulation has been considered in the past as a useful and versatile tool for investigating several aspects of both fixed- and rotary-wing vehicle dynamics, Thomson & Bradley (2006). A wide plethora of methods for solving inverse simulation problems in flight mechanics has been considered, that can be broadly grouped into three major categories: (i) differential methods, Kato & Sugiura (1986), suitable for nominal problems only, where the number of control inputs equals that of tracked variables; (ii) integration methods, Hess & Gao (1991), where the required control action is evaluated over a discrete time interval and can handle also redundant problems (e.g. by means of a local optimization approach, De Matteis et al. (1995)); and (iii) global methods, where the time-history of the control variable is determined over the whole duration of the tracked maneuver by means of a variational approach, Borri et al. (1997).

An integration approach is here applied, which is derived from an algorithm that was successfully applied to the evaluation of helicopter handling qualities, Avanzini et al. (2013). In this respect, three different maneuvers are considered. In the first two case, a U turn and a 360 deg yaw rotation in forward flight, the behavior of the novel configuration is compared with that of an equivalent conventional quad-rotor. The third maneuver, a 90 deg roll rotation in forward flight, represents a test case that can be flown only if the rotors are allowed to tilt. This maneuver represents a severe challenge and it fully demonstrates that the tilting rotors provide the vehicle with a significantly expanded maneuver envelope.

2. DERIVATION OF THE EQUATIONS OF MOTION

The quad-rotor under consideration consists of a rigid cross frame equipped with four rotors as shown in Fig. 1.a. The model is derived under the assumptions that motor and rotor response is fast and their dynamics can therefore be neglected. Also, rotor blades are assumed to be rigid (i.e. no blade flapping occurs). As outlined above, control moments can be obtained either differentially changing the value of thrust and torque of each rotor changing its angular speed or tilting the rotor so that thrust can be projected into a horizontal and a vertical component in the body frame. The configuration of the quad-rotor with all the rotors tilted is shown in Fig. 1.b.

The equations of motion are developed in terms of the translational and rotational velocities represented in body-frame components, $\boldsymbol{v}_b$ and $\boldsymbol{\omega}_b$, where attitude is represented using quaternions, $(q_0, \boldsymbol{q}^T)^T$, Wertz (1978):

$$\dot{\boldsymbol{v}}_b = -\boldsymbol{\omega}_b \times \boldsymbol{v}_b + \frac{\boldsymbol{F}}{m} + \boldsymbol{g}_b \tag{1}$$

$$\dot{\boldsymbol{\omega}}_b = \boldsymbol{J}^{-1}\left[\boldsymbol{M} - \boldsymbol{\omega}_b \times (\boldsymbol{J}\boldsymbol{\omega}_b)\right] \tag{2}$$

$$\dot{q}_0 = -\frac{1}{2}\boldsymbol{\omega}_b \cdot \boldsymbol{q} \tag{3}$$

$$\dot{\boldsymbol{q}} = \frac{1}{2}\left(q_0\boldsymbol{\omega}_b - \boldsymbol{\omega}_b \times \boldsymbol{q}\right) \tag{4}$$

$$\dot{\boldsymbol{r}}_i = \boldsymbol{T}_{bi}\boldsymbol{v}_b \tag{5}$$

where $\boldsymbol{F}$ and $\boldsymbol{M}$ indicate aerodynamic force and moments, respectively, $\boldsymbol{g}_b$ is gravity acceleration, $\boldsymbol{J}$ is the inertia tensor, and $\boldsymbol{T}_{bi}(q_0, \boldsymbol{q}^T)$ is the coordinate transformation matrix from inertial to body frame.

The use of quaternions for attitude representation allows the simulation of more aggressive maneuvers, that requires unusual pitch attitude that cannot be represented using Euler angles. The aerodynamic force acting on the quad-rotor $\boldsymbol{F}$ is given by the difference between rotor thrust and vehicle drag:

$$\boldsymbol{F} = \boldsymbol{T} - \boldsymbol{D} \tag{6}$$

Letting $\mathrm{s}\delta_i = \sin\delta_i$ and $\mathrm{c}\delta_i = \cos\delta_i$, it is

$$\boldsymbol{T} = k_t \begin{bmatrix} 0 & \mathrm{s}(\delta_2) & 0 & -\mathrm{s}(\delta_4) \\ \mathrm{s}(\delta_1) & 0 & -\mathrm{s}(\delta_3) & 0 \\ -\mathrm{c}(\delta_1) & -\mathrm{c}(\delta_2) & -\mathrm{c}(\delta_3) & -\mathrm{c}(\delta_3) \end{bmatrix} \begin{Bmatrix} \Omega_1^2 \\ \Omega_2^2 \\ \Omega_3^2 \\ \Omega_4^2 \end{Bmatrix} \tag{7}$$

Drag is considered only for the quad-rotor body. The body is assumed to be a prism with a square base. Following Heffley (1986), the components of the drag force can be expressed as

$$\boldsymbol{D} = \frac{1}{2}\rho \left\{ \begin{array}{c} C_{dx} S_x V_{bx}^2 \\ C_{dy} S_y V_{by}^2 \\ C_{dz} S_z V_{bz}^2 \end{array} \right\} \tag{8}$$

with $C_{dx} = C_{dy} = 0.8$ and $C_{dz} = 1.05$, Hoerner (1965). Similarly the moment applied on the quad-rotor is defined as

$$\boldsymbol{M} = \left(k_t \frac{b}{2} \left[\begin{array}{cccc} 0 & -\mathrm{c}\delta_2 & 0 & \mathrm{c}\delta_4 \\ -\mathrm{c}\delta_1 & 0 & \mathrm{c}\delta_3 & 0 \\ \mathrm{s}\delta_1 & \mathrm{s}\delta_2 & -\mathrm{s}\delta_3 & -\mathrm{s}\delta_4 \end{array} \right] + k_c \left[\begin{array}{cccc} 0 & \mathrm{s}(\delta_2) & 0 & \mathrm{s}(\delta_4) \\ \mathrm{s}(\delta_1) & 0 & \mathrm{s}(\delta_3) & 0 \\ -\mathrm{c}(\delta_1) & \mathrm{c}(\delta_2) & \mathrm{c}(\delta_3) & -\mathrm{c}(\delta_4) \end{array} \right] \right) \left\{ \begin{array}{c} \Omega_1^2 \\ \Omega_2^2 \\ \Omega_3^2 \\ \Omega_4^2 \end{array} \right\} \tag{9}$$

The control inputs modify the variation of rotor angular rate and tilt angle. Letting

$$\boldsymbol{\delta} = \left[\begin{array}{ccc} 1 & 0 & 1 \\ 1 & 1 & 0 \\ 1 & 0 & -1 \\ 1 & -1 & 0 \end{array} \right] \left\{ \begin{array}{c} w_1 \\ w_2 \\ w_3 \end{array} \right\} \tag{10}$$

and $\boldsymbol{U}_\Omega = (\Omega_1, \Omega_2, \Omega_3, \Omega_4)^T = \boldsymbol{U}_{\Omega_0} + \boldsymbol{\Delta\Omega}$, with

$$\boldsymbol{\Delta\Omega} = \Omega_0 \left[\begin{array}{cccc} 1 & 0 & 1 & 1 \\ 1 & 1 & 0 & -1 \\ 1 & 0 & -1 & 1 \\ 1 & -1 & 0 & -1 \end{array} \right] \left\{ \begin{array}{c} u_1 \\ u_2 \\ u_3 \\ u_4 \end{array} \right\} \tag{11}$$

the vector of control inputs is given by
$u = (u_1, u_2, u_3, u_4, w_1, w_2, w_3)^T$.

With respect to the control inputs of a conventional single main rotor helicopter, it is possible to notice that the variation of u_1 increases overall rotor thrust and it is thus equivalent to a collective command; u_2 and w_2 provide longitudinal control moments (that is, they are equivalent to a longitudinal cyclic pitch variation), whereas u_3 and w_3 develop a roll control moment, equivalent to the effect of lateral cyclic; finally u_4 and w_1 represent yaw commands, that substitute tail rotor pitch.

Inverse Simulation Algorithm

As anticipated in the Introduction, the IS problem is solved by means of an integration algorithm Hess & Gao (1991); De Matteis et al. (1995). When quad-rotor dynamics is expressed in terms of a set of nonlinear ordinary differential equations, it can be represented in compact form as

$$\dot{\boldsymbol{x}} = \boldsymbol{f}(\boldsymbol{x}, \boldsymbol{u}) \; ; \quad \boldsymbol{y} = \boldsymbol{g}(\boldsymbol{x}) \tag{12}$$

where a dot indicates the time derivative, $\boldsymbol{x} = (\boldsymbol{V}_b^T, \boldsymbol{\omega}_b^T, q_0, \boldsymbol{q}^T, \boldsymbol{r}^T)^T \in \mathbb{R}^n$ is the state vector (with $n = 13$), $\boldsymbol{u} = (u_1, u_2, u_3, u_4, w_1, w_2, w_3)^T \in \mathbb{R}^m$ is the vector of $m = 7$ control variables presented in the previous paragraph for this unconventional configuration. Finally $\boldsymbol{y} \in \mathbb{R}^p$ is the vector of tracked output variables.

Once a desired variation with time of the output, $\boldsymbol{y}_{des}(t)$, is available, equations of motion are integrated from an initial condition $\boldsymbol{x}_I = \boldsymbol{x}_k$ at time t_k over a time interval Δt for a piece-wise constant value $\boldsymbol{u}_k^\star$ of the control variables. The resulting value $\boldsymbol{y}_F = \boldsymbol{g}(\boldsymbol{x}_F)$ of the output variables at time $t_F = t_{k+1} = t_k + \Delta t$ is thus a function of the (given) initial state $\boldsymbol{x}_k$ and of the (unknown) constant control action, $\boldsymbol{u}_k^\star$.

Control variables can then be determined in such a way that $\boldsymbol{y}_F$ matches the value of $\boldsymbol{y}_{des}$ at time t_F, that is, the inverse problem can be stated in terms of a set of p algebraic equations in the form

$$\boldsymbol{y}_F = \boldsymbol{F}(\boldsymbol{x}_k, \boldsymbol{u}_k^\star) = \boldsymbol{y}_{des}(t_F) \tag{13}$$

with m unknowns. When $m = p$, the problem is nominal and, if well posed, it can be solved by means of standard numerical techniques, such as Newton-Raphson (NR) method, Hess & Gao (1991). If $m > p$ the problem is redundant, as in many aeronautical applications for fixed and rotary-wing aircraft. When the redundancy degree is $m - p = 1$, as for the conventional quad-rotor, where $\boldsymbol{u} = (u_1, u_2, u_3, u_4)^T \in \mathbb{R}^4$, one additional constraint is sufficient for making the problem nominal, where a desired value of a relevant parameter can be enforced in order to obtain trajectories with an additional desired feature (*e.g.* zero lateral acceleration or zero sideslip).

In the present case, the presence of 3 additional degrees of freedom makes the system highly redundant. This marks a major difference between the standard and the novel configuration, where the conventional quad-rotor features four controls that are used to track three desired trajectory variables plus an additional constraint. The resulting nominal inverse simulation problem is solved using a Newton-Raphson algorithm. Conversely, the novel configuration features 7 control variables and this requires a different approach for the solution of the inverse problem.

Hess & Gao (1991) proposed a solution method for redundant problems based on the use of the so-called Moore-Penrose pseudo-inverse during NR iterations, which results into the minimum-norm control vector that solves the problem. A more general approach was proposed in De Matteis et al. (1995), where an optimization problem is solved in order to enforce, together with the constraints on trajectory variables, relevant properties to the inverse solution by defining a suitable merit function to be minimized locally at each time step of the inverse simulation. In the present case, the inverse simulation step is solved using a sequential programming (SQP) numerical optimization algorithm that, in addition to the constraints defined as for the conventional configuration, also minimizes the control effort on command variables u_2, u_3 and u_4, and deviations from desired values for roll and pitch angles.

A further problem with aeronautical applications of IS integration methods is represented by undesirable oscillations in the control action or even instabilities in the inverse solution, discussed in some details in Thomson & Bradley (2006); Lin et al. (1993); Yip & Leng (1998); Lin (1993), that may be due to uncontrolled states and/or numerical issues in the evaluation of the output Jacobian matrix $\boldsymbol{J} = \partial \boldsymbol{y}_F / \partial \boldsymbol{u}_k^\star$. These issues can be circumvented, at the cost of increasing the computational burden, by

solving the inverse problem stated by Eq. (13) over a longer time-horizon, that is, choosing $t_F^\star = t_k + N\Delta t > t_{k+1}$, that is, the piece-wise constant control action is propagated for a longer time interval in order to allow for uncontrolled dynamics to settle down. The initial condition $\boldsymbol{x}_{k+1}$ for the next step is then evaluated at time t_{k+1}, as in De Matteis et al. (1995).

As a variation to a standard integration method, a different definition of the algebraic system is adopted in this paper, where, rather than solving Eq. (13) in terms of the actual value of the tracked variables at time t_F, their increments over the time step between t_I and $t_F^\star$ are required to be equal. Equation (13) is thus replaced with

$$\begin{aligned}\Delta\boldsymbol{y} = \boldsymbol{F}(\boldsymbol{x}_k, \boldsymbol{u}_k^\star) - \boldsymbol{g}(\boldsymbol{x}_k) = \\ = \boldsymbol{y}_{des}(t_F) - \boldsymbol{y}_{des}(t_I) + K\left[\boldsymbol{y}_{des}(t_I) - \boldsymbol{g}(\boldsymbol{x}_k)\right]\end{aligned} \tag{14}$$

where the additional term in square brackets multiplied by a gain K avoids that the actual solution "drifts" away from the desired path because of the incomplete implementation of the considered step during the forward propagation, as outlined above. This term also enforces asymptotic convergence on the tracked variables when they achieve a steady value. By some simple manipulation, Eq. (14) can be rearranged as

$$\boldsymbol{F}(\boldsymbol{x}_k, \boldsymbol{u}_k^\star) = \boldsymbol{y}_{des}(t_F) + (K-1)\left[\boldsymbol{y}_{des}(t_I) - \boldsymbol{g}(\boldsymbol{x}_k)\right] \tag{15}$$

where for $K = 0$ the additional term disappears and one simply requires that the increment of the actual output variables at the end of the whole inverse simulation step $\Delta t = t_F - t_I$ equals the increment for the desired variation of $\boldsymbol{y}$, whereas for $K = 1$ the original formulation of Eq. (13) for the inverse problem is recovered.

This is the most general inverse simulation scheme implemented, unless otherwise stated. Only for the last test case a few difference will be pointed out when discussing the results for the roll tilt maneuver.

3. RESULTS

Geometrical characteristics and other model parameters used for describing quad-rotor dynamics are summarized in Table 1.

Table 1. Quadrotor data

Data	Symbol	Value	Unit
Mass	m	0.941	kg
Rotor radius	R	0.127	m
Rotor distance from c.g.	b	0.465	m
Height	h	0.08	m
Width	d	0.1	m
Inertia moments	$J_{xx} = J_{yy}$	0.0121	kg m^2
	J_{zz}	0.0018	kg m^2
Rotor rate at hovering	Ω_0	382.06	rad/s
Thrust constant	k_t	$1.581 \cdot 10^{-5}$	-
Torque constant	k_c	$4.16 \cdot 10^{-7}$	-

The inverse simulation algorithm is tested on 3 different maneuvers: a U turn, a 360° yaw turn in straight flight, and a 90° roll tilt in forward flight. Table 2 summarizes data used to define the test cases. All the maneuvers start from a hovering condition, so that an initial acceleration is always included. A graphical representation of the desired variation of the most relevant tracked outputs for the three maneuvers are reported in Figs. 2-4.

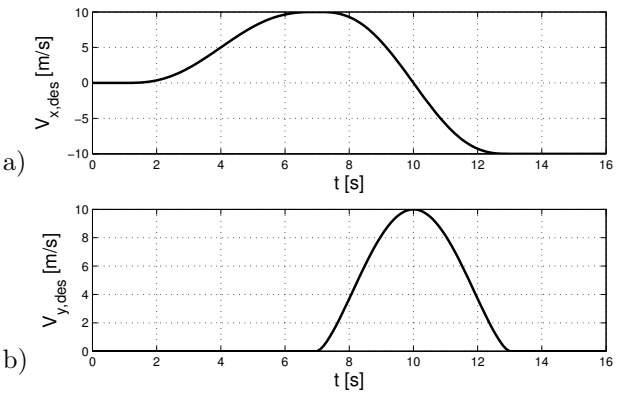

Fig. 2. U-turn: desired x (a) and y (b) inertial speed.

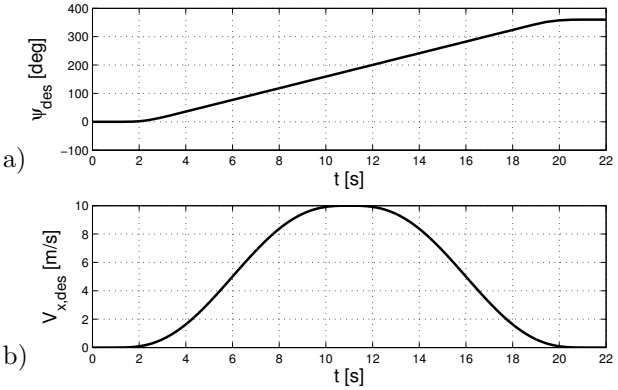

Fig. 3. Yaw rotation: desired ψ (a) and x inertial speed (b).

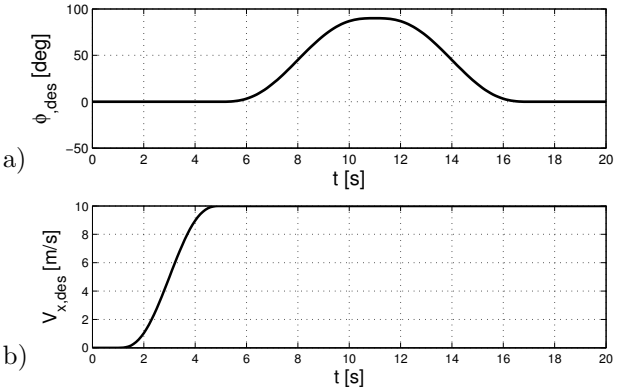

Fig. 4. Roll tilt: desired ϕ (a) and x inertial speed (b).

Table 2. Test cases characteristics

Test case	Duration	Tracked outputs
U turn	16s	$V_{x,d}, V_{y,d}$
360° yaw turn	22 s	$r, V_{x,d}$
90° roll tilt	20 s	$\phi, V_{x,d}$

For the first two test cases the results obtained for the tilting rotor configuration are compared with those of a standard configuration. The third maneuver cannot be tracked by a conventional quad-rotor, which is thus not considered. For all the maneuvers the inverse simulation algorithm determines a piece-wise constant control over a

time step $\Delta t = 0.1$ s, but the inverse problem is solved over a longer interval, $N\Delta t = 0.2$ s.

3.1 U turn maneuver

The first maneuver is a U turn starting from hover. The quad-rotor initially accelerates in the x inertial direction, then it reverts its direction of flight. The desired variation of V_x velocity is obtained using a fifth order polynomial in order to have C^2 continuity at the bounds of the time intervals in which the maneuver is divided (acceleration, turn, forward flight in the reverse direction), whereas V_y is kept equal to zero during the acceleration and final straight flight:

$$
\begin{aligned}
&t < 1, && V_{x,d} = 0, V_{y,d} = 0 \\
&1 < t < T/2, && V_{x,d} = \tilde{V}\left(10\tau^3 - 15\tau^4 + 6\tau^5\right), V_{y,d} = 0 \\
&T/2 < t < T-1, && \\
&\quad V_{x,d} = \tilde{V}\left(63 - 240\tau + 360\tau^2 - 260\tau^3 + 90\tau^4 - 12\tau^5\right) && \\
&\quad V_y = (\tilde{V}^2 - V_x^2)^{-1/2} && \\
&t > T-1, && V_{x,d} = -\tilde{V}, V_{y,d} = 0
\end{aligned}
$$

where τ is the nondimensional time

$$\tau = 2\frac{t-1}{T-2} \tag{16}$$

and T is the total simulation time. During the whole maneuver the sideslip angle is maintained as small as possible.

Figures 5 to 9 show the results for this test case. The variation of inertial speed components (V_x, V_y, and V_z) are presented in figure 5. Velocity components in the horizontal plane are tracked with acceptable errors by both the conventional quad-rotor and the configuration with tilting rotors. Conversely, the speed component along the vertical (z) axis presents more significant errors when the conventional configuration is considered. In figure 6 the sideslip velocity (v) is shown. It is evident that, during the maneuver, the novel configuration does not maintain the desired zero-sideslip condition with the same accuracy achieved by the standard quad-rotor. This is a side effect of the local optimization process, where pitch and roll angle (θ and ϕ, shown in Fig. 7), are kept as small as possible, together with u_2, u_3, and u_4 control variables. When the quad-rotor performs a flat turn with $\phi \approx 0$, a perfectly zero-sideslip condition cannot be maintained. When minor variations of the roll angle are allowed, the sideslip angle drops back almost exactly to zero.

Figure 8 represents the variation of commands on rotor angular speed, u_i, $i = 1, 2, 3, 4$, as defined in eq. (11). As expected, these commands are significantly smaller when tilting rotor are employed. Only the collective rotor speed command is significantly different from zero. Figure 9 shows rotors tilt angles for the tilting rotor case. Large variations of rotor inclination take the place of quad-rotor attitude angles, a feature that potentially increases the effectiveness of the novel configuration for observation of targets on the ground, provided that a camera mounted on the vehicle would not undergo large rotations associated to vehicle maneuver state.

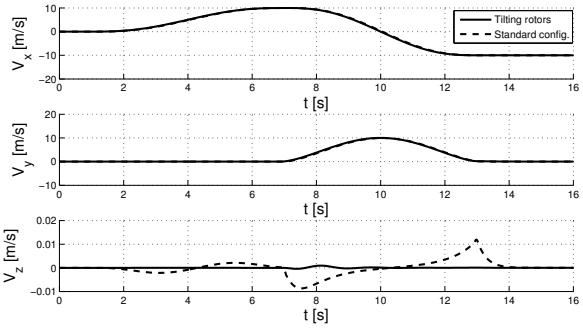

Fig. 5. Inertial speeds for the U turn maneuver, comparison between the standard case (dashed line) and the tilting rotor configuration (solid line)

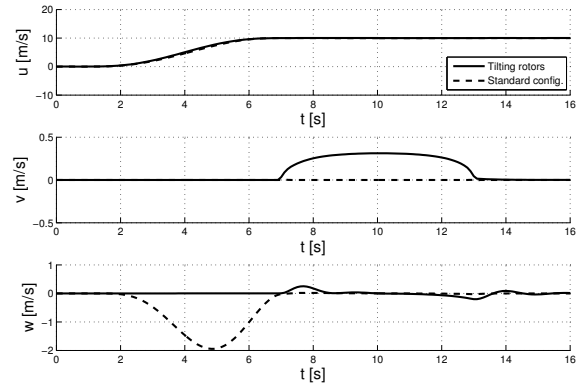

Fig. 6. Body speeds for the U turn maneuver, comparison between the standard case (dashed line) and the tilting rotor configuration (solid line)

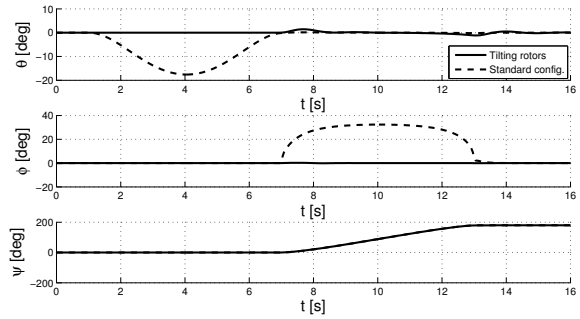

Fig. 7. Euler angles variation for the U turn maneuver, comparison between the standard case (dashed line) and the tilting rotor configuration (solid line)

3.2 360° yaw turn straight flight

The second maneuver starts again from hover. The quad-rotor is required to increase its speed along the inertial x direction, during the first half of a full 360° yaw rotation, while it must decelerate back to hover while completing the second half of the rotation. In this maneuver the controlled variables are the longitudinal inertial speed component V_x and the yaw rate r. The prescribed variations of these variables are

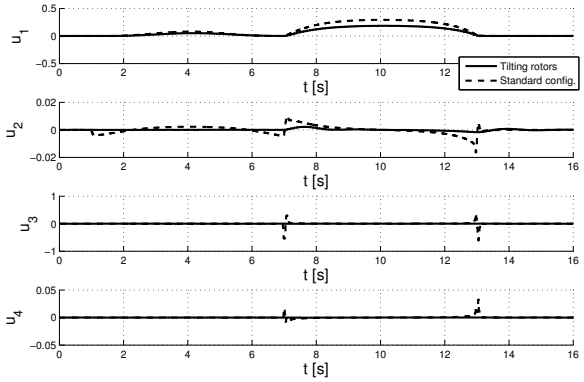

Fig. 8. Rotor speed commands for the U turn maneuver, comparison between the standard case (dashed line) and the tilting rotor configuration (solid line)

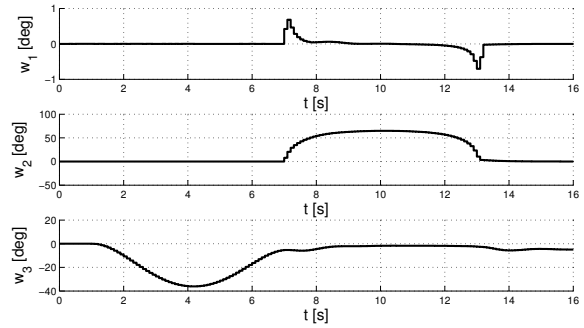

Fig. 9. Tilting rotors angle command for the U turn maneuver

$$
\begin{aligned}
&t < 1, && V_{x,d} = 0, \quad r_d = 0 \\
&1 \le t < T/8, && V_{x,d} = \tilde{V}\left(10\tau^3 - 15\tau^4 + 6\tau^5\right) \\
& && r_d = \tilde{r}\left(640\tau^3 - 3840\tau^4 + 6144\tau^5\right) \\
&1 < t < T/2, && V_{x,d} = \tilde{V}\left(10\tau^3 - 15\tau^4 + 6\tau^5\right) \\
& && r_d = \tilde{r} \\
&T/2 < t < 7T/8 && \\
& V_{x,d} = \tilde{V}\left(32 - 120\tau + 180\tau^2 - 130\tau^3 + 45\tau^4 - 6\tau^5\right) && \\
& r_d = \tilde{r} && \\
&T/8 < t < T/1 && \\
& V_{x,d} = \tilde{V}\left(32 - 120\tau + 180\tau^2 - 130\tau^3 + 45\tau^4 - 6\tau^5\right) && \\
& r_d = \tilde{r}\left(140288 - 376320\tau + 403200\tau^2 - 215680\tau^3 + \right. && \\
& \qquad \left. + 57600\tau^4 - 6144\tau^5\right) && \\
&t > T - 1, && V_{x,d} = 0, \quad r_d = 0
\end{aligned}
$$

where τ is defined as in eq. (16) and $T = 22s$.

Figures 10 to 13 present vehicle response and commands. Desired velocity and yaw angle are tracked by both quad-rotor models, but roll and pitch angles exhibit an undesired oscillatory response for the standard configuration. Vertical inertial speed component remain close to zero in both cases, whereas lateral deviations are more significant when the novel configuration is adopted, but this is the cost associated to keeping roll and pitch attitude close to zero, in order to maintain an almost perfectly horizontal attitude during the yaw rotation.

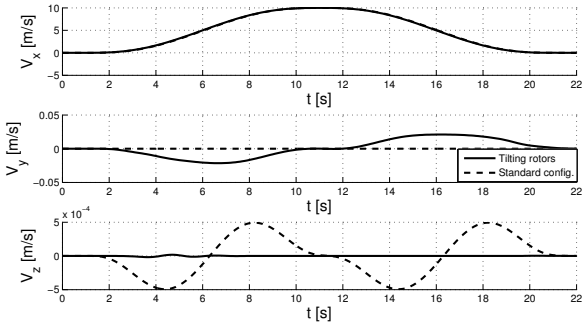

Fig. 10. Inertial speed for the 360° yaw turn maneuver, comparison between the standard case (dashed line) and the tilting rotor configuration (solid line)

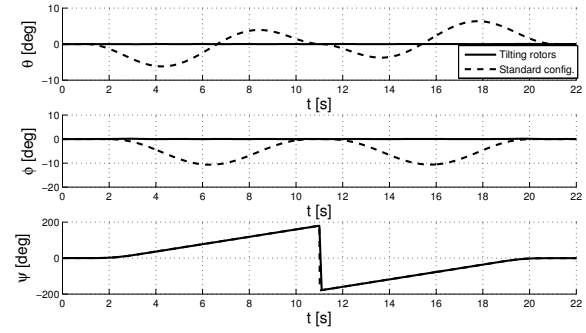

Fig. 11. Euler angle variations for the 360° yaw turn maneuver, comparison between the standard case (dashed line) and the tilting rotor configuration (solid line)

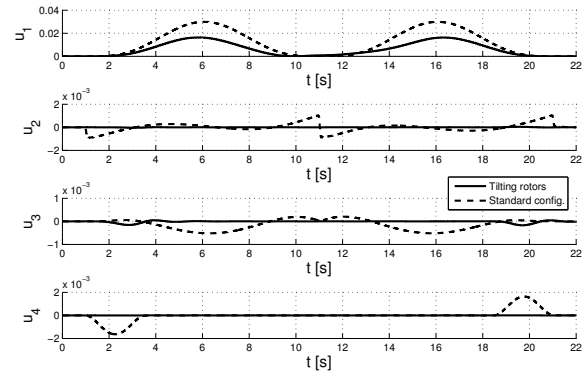

Fig. 12. Rotor speed command for the 360° yaw turn maneuver, comparison between the standard case (dashed line) and the tilting rotor configuration (solid line)

Note that the yaw command needed to perform a complete yaw rotation are small for both models (see u_4 control for the standard configuration in Fig. 12 and command w_1 for the quad-rotor with tilting rotors case in Fig. 13). This is due to two different reasons. On one side a low-speed maneuver is considered where aerodynamic drag and moments remain small. At the same time, no aerodynamic force in the rotor plane is included in this simple model, where rotors develop only a thrust component in the direction normal to the rotor disk. This means that aerodynamic yaw damping moments are largely underestimated.

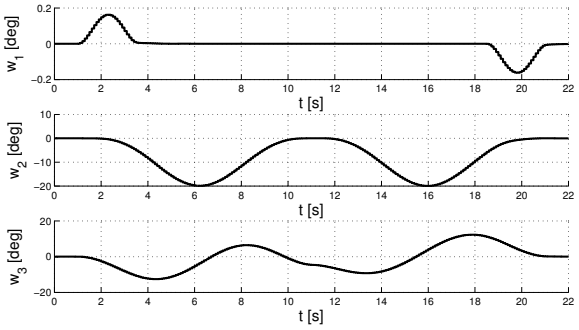

Fig. 13. Tilting rotors angle command for the 360° yaw turn maneuver, comparison between the standard case (dashed line) and the tilting rotor configuration (solid line)

3.3 90° roll tilt

The third maneuver demonstrates a maneuver capability that is simply unachievable for a conventional quad-rotor. For this reason, only the tilting-rotor model is here considered. The longitudinal inertial velocity component V_x is initially incremented from hover to a desired value, $\tilde{V}$. Meanwhile the desired roll angle ϕ is incremented from 0 to 90° and then brought back to 0°. This maneuver can be useful when the quad-rotor needs to cross a narrow vertical opening or passage, so that it is necessary to tilt it 90° while flying along a straight trajectory.

Desired inertial velocity and roll angle are defined again using 5th order polynomials:

$$
\begin{aligned}
&t < 1, && V_{x,d} = 0, \quad \phi_d = 0 \\
&1 < t < T/4, && V_{x,d} = \tilde{V}\left(80\tau^3 - 240\tau^4 + 192\tau^5\right) \\
& && \phi_d = 0 \\
&T/4 \le t < 5/8T, && V_{x,d} = \tilde{V} \\
& && \phi_d = \tilde{\phi}\left(-6.71 + 49.38\tau - 138.27\tau^2 + 181.73\tau^3 + \right. \\
& && \left. \quad -110.62\tau^4 + 25.28\tau^5\right) \\
&5/8T \le t < T-1, && V_{x,d} = \tilde{V} \\
& && \phi_d = \tilde{\phi}\left(240.20 - 790.12\tau + 1027.16\tau^2 - 655.80\tau^3 + \right. \\
& && \left. \quad +205.43\tau^4 - 25.28\tau^5\right) \\
&t > T-1, && V_{x,d} = \tilde{V}, \quad \phi_d = 0
\end{aligned}
$$

with τ defined as in eq. (16), and $T = 20\,\mathrm{s}$.

The inverse simulation algorithm used in this case is slightly different from that used for other maneuvers. Provided that precise tracking of the roll angle is not required, as minor discrepancies in this variable with respect to the desired value would not affect the result, the guidance term in the definition of the desired increment of ϕ was removed. In this case Eq. (15) for the roll angle ϕ is thus modified and it is implemented in the form

$$\boldsymbol{F}_\phi(\phi_k, \boldsymbol{u}_k^\star) = \phi_d(t_F) - \phi_d(t_I) + \boldsymbol{g}(\boldsymbol{x}_k) \qquad (17)$$

Figures 14 to 17 present the results obtained for this last case. The vehicle follows the desired inputs, for both velocity and roll angle with satisfactory accuracy (velocity components and roll angle).

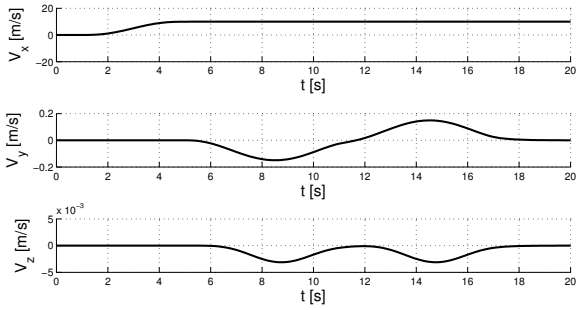

Fig. 14. Inertial speed for the 90° roll tilt maneuver

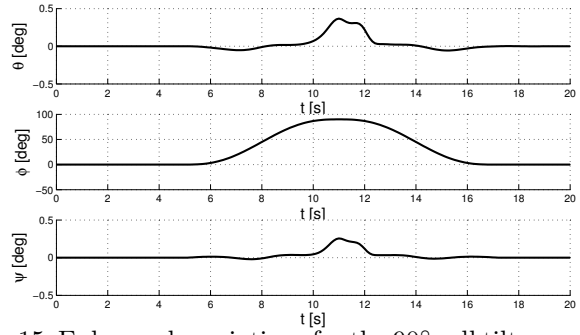

Fig. 15. Euler angle variations for the 90° roll tilt maneuver

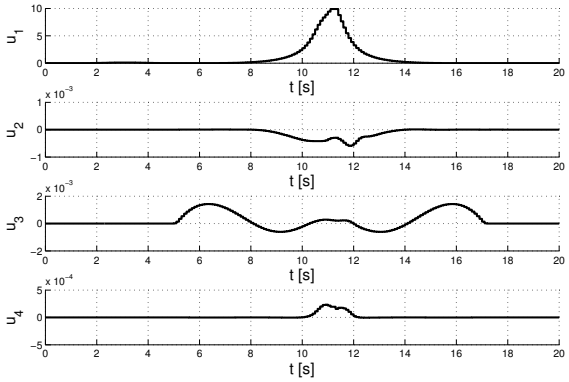

Fig. 16. Rotor speed command for the 90° roll tilt maneuver

The commands needed to perform the maneuver are reported in Figs. 16 and 17. The variations in rotor angular rates are kept small (Fig. 16). Only the "collective" command u_1 is increased when the quad-rotor is completely tilted, which is clearly required by the need for providing enough lift force using only two rotors, in order to maintain the required straight flight condition at constant altitude. As for the other commands on tilt angles (Fig. 17), one can note that the maneuver starts with a small increment for w_3 that accelerates the vehicle in the x-direction, than w_2 takes over and this command provides most of the control power for performing the unconventional roll maneuver in forward flight, where rotors 1 and 3 are tilted for most of the duration of the maneuver.

4. CONCLUSIONS

A novel quad-rotor configuration that features tilting rotors was analyzed in order to assess the maneuvering potential of the vehicle and possible advantages over

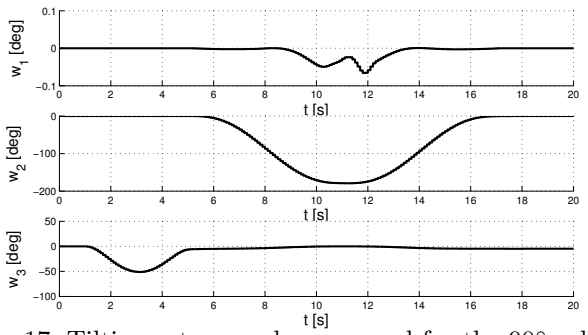

Fig. 17. Tilting rotors angle command for the 90° roll tilt maneuver

conventional quad-rotors. When the two configurations are compared, it is shown that tilting the rotors provides a larger control power that allows to maintain a constant rotor rate. This would allow for the use of constant RPM variable pitch rotors instead of fixed pitch, variable RPM propellers. In the former case rotor thrust is controlled by means of propeller pitch, which results in a more efficient propulsion system.

Moreover, the inverse simulation algorithm used for tracking three different maneuvers demonstrates that it is possible to use the additional control degrees of freedom for either minimizing the control effort or for flying with unconventional attitude, that range from a simple horizontal attitude in forward flight (instead of the usual pitch down attitude of standard quadcopters) to more demanding transition to 90 deg roll attitude in forward rectilinear flight.

REFERENCES

G. Avanzini, G. De Matteis, and A. Torasso, Modelling Issues in Helicopter Inverse Simulation, *36th European Rotorcraft Forum ERF 2010*, Paris, France, 7-9 September 2010.

G. Avanzini, and F. Giulietti, Quadcopter configuration with tilting rotors, Pat. WO2013098736 A2, request No. PCT/IB2012/057589, Dec. 2012.

G. Avanzini, D. Thomson, and A. Torasso, Model Predictive Control Architecture for Rotorcraft Inverse Simulation *Journal of Guidance, Control & Dynamics*, Vol. 36, No. 1, 2013, pp. 207-217.

M. Borri, C. L. Bottasso, and F. Montelaghi, Numerical Approach to Inverse Flight Dynamics, *Journal of Guidance, Control & Dynamics*, Vol. 20, No. 4, Jul.-Aug. 1997, pp. 742-747.

G. De Matteis, L. M. De Socio, and A. Leonessa, Solution of aircraft inverse problems by local optimization, *Journal of Guidance, Control & Dynamics*, Vol. 18, No. 3, May-Jun. 1995, pp. 567-571.

R. H. Heffley, and M. A. Mnich, Minimum complexity helicopter simulation math model, *Contract NAS2-11665, Muadyne Report 83-2-3*, Ames Research Center, October 1986.

R. A. Hess, C. Gao, and S. H. Wang, Generalized technique for inverse simulation applied to aircraft manoeuvres, *Journal of Guidance, Control & Dynamics*, Vol. 14, No. 5, Sep.-Oct. 1991, pp. 920-926.

S. F. Hoerner, *Fluid-Dynamic Drag*, Hoerner Fluid Dynamic, 1965.

G. M. Hoffmann, H. Huang, S. L. Waslander, and C. J. Tomlin, Precision flight control for a multi-vehicle quadrotor helicopter testbed, *Control Engineering Practice*, 2011.

O. Kato, and I. Sugiura, An interpretation of airplane general motion and control as inverse problem, *Journal of Guidance, Control& Dynamics*, Vol. 9, No. 2, Mar.-Apr. 1986, pp. 198-204.

F. Kendoul, Survey of advances in guidance, navigation, and control of unmanned rotorcraft systems, *Journal of Field Robotics*, 2012.

K. C. Lin, Comment on 'Generalized Technique for Inverse Simulation Applied to Aircraft Maneuvers', *Journal of Guidance, Control & Dynamics*, Vol.16, No. 6, Nov.-Dec. 1993, pp. 1196-1197.

K. C. Lin, P. Lu, and M. Smith, The Numerical Errors in Inverse Simulation, *AIAA Paper 93-3588*, Aug. 1993.

N. Michael, D. Scaramuzza, and V. Kumar, Special issue on micro-UAV perception and control, *Autonomous Robots*, 2012.

P. Pounds, R. Mahony, and P. Corke, Modelling and Control of a Large Quadrotor Robot, *Control Engineering Practice*, 2010.

E. Stingu, and F. Lewis, Design and Implementation of a Structured Flight Controller for a 6DoF Quadrotor Using Quaternions, *17th Mediterranean Conference on Control & Automation*, Makedonia Palace, Thessaloniki, Greece, June 24 - 26, 2009.

D.G. Thomson, and R. Bradley, Inverse simulation as a tool for flight dynamics research: Principles and applications, *Progress in Aerospace Sciences*, Vol. 42, No. 3, May 2006, pp. 174-210.

J.R. Wertz, *Spacecraft Attitude Determination and Control*, Springer, 1978, pp. 758–760.

K. M. Yip, and G. Leng, Stability analysis for inverse simulation of aircraft, *Aeronautical Journal*, Vol . 102, No. 1016, 1998, pp. 345-351.